

Antibacterial efficacy of zinc oxide nanoparticles synthesized by green and chemical methods

Arwa Al Bustany¹, Hassan Abbas¹, Abd Al-Naser Al-Omar², Alaa Mohamad Sobh³, Thanaa Shriteh⁴, Hashem AL Mahfoud⁵

¹Department of Animal Production, Faculty of Agriculture, Al-Baath University, Homs, Syria

²General Commission for Scientific Agricultural Research, Hama Research Center, Hama, Syria

³Department of Food Technology, Faculty of Technical Engineering, University of Tartous, Tartous, Syria

⁴Department of Chemistry, Faculty of Science, Albaath University, Homs, Syria

⁵Department of Renewable Energy Technologies, Faculty of Technical Engineering, University of Tartous, Tartous, Syria

Abstract

Background: Zinc oxide (ZnO) as an antimicrobial and non-toxic agent has been widely explored in comparison with other materials. The green manufacturing of mineral nanoparticles using plant extracts has outperformed other manufacturing methods due to many advantages.

Methods: ZnO nanoparticles (ZnO NPs) were synthesized using two distinct methods: chemical synthesis and a green method involving lemon leaf extract. The synthesized ZnO was characterized using UV-Vis, X-ray diffraction (XRD), scanning electron microscope (SEM), and Fourier transform infrared spectroscopy (FTIR) analyses. The antibacterial activity of the resulting ZnO NPs was evaluated against two gram-negative bacterial strains, *Escherichia coli* and *Pseudomonas aeruginosa*, and one gram-positive strain, *Staphylococcus aureus*, using the etching diffusion method.

Results: In this study, ZnO NPs were synthesized using a green method from an inexpensive and readily available source, lemon leaf extract, and compared with those synthesized by a chemical method. The results showed that ZnO NPs obtained via the green synthesis method had a semi-spherical shape with an average size of 14.25 nm, which is smaller than the average size of chemically synthesized ZnO NPs at 34 nm. The effectiveness of the ZnO NPs varied depending on the bacterial strain tested. Gram-positive bacteria were more sensitive than gram-negative bacteria.

Conclusion: ZnO NPs produced from lemon leaf extract were most effective against *S. aureus*. Chemically synthesized ZnO NPs were more effective against gram-negative bacteria.

Keywords: Zinc oxide, Plant extracts, Anti-bacterial agents, *Staphylococcus*

Citation: Al Bustany A, Abbas H, Al-Omar AAN, Sobh A, Shriteh T, AL Mahfoud H. Antibacterial efficacy of zinc oxide nanoparticles synthesized by green and chemical methods. Environmental Health Engineering and Management Journal 2024; 11(4): 409-418 doi: 10.34172/EHEM.2024.40.

Article History:

Received: 8 May 2024

Accepted: 26 August 2024

ePublished: 2 October 2024

*Correspondence to:

Alaa Sobh,

Email: Alaasobh@tartous-univ.edu.sy

Introduction

Nanotechnology is a science that uses various techniques to synthesize nanoparticles with a larger surface area that possess unique behavior and special properties (1,2). This is useful because many important electrical and chemical reactions occur only on surfaces and are sensitive to the surface's texture and shape as well as its chemical composition (3,4).

Progress in the field of nanotechnology has included many fields, including pharmacology, embryology, medicine, and many other fields (5). These nanoparticles are manufactured in several ways, including physical, chemical, or biological methods. In recent years, the green manufacturing of mineral nanoparticles using plant extracts has outperformed other manufacturing methods due to many advantages, including low cost, effectiveness,

and environmental safety (6). Metal nanoparticles prepared using plant extracts are also characterized by high stability and require less time for reduction. The main reasons that make this method environmentally friendly are the safe solvents, reference agents, and non-toxic materials used, and it can be easily scaled up to produce larger quantities and there is no need to use high pressure, energy, or dangerous chemicals (7). It is one of the most important nanomaterials that have been widely used in recent times. Metal oxides such as zinc oxide (ZnO), Fe₂O₃, Ag₂O, MgO, and CuO, have been proven as effective antibacterial agents (8).

ZnO has been widely explored in comparison with other materials as an antimicrobial and non-toxic agent, showing bactericidal properties on gram-positive and gram-negative bacteria, including *Escherichia*



coli, *Salmonella enteritidis*, *Streptococcus pyogenes*, *Aeromonas hydrophila*, *Bacillus subtilis*, *Staphylococcus aureus*, *Listeria monocytogenes*, *Klebsiella pneumonia*, *Pseudomonas aeruginosa*, *Salmonella typhimurium*, *Enterococcus faecalis*, etc (9). Moreover, it has been recognized by the US Food and Drug Administration as a safe substance (GRAS) (10).

Lemon is an evergreen tree, belonging to the Rutaceae family (11); studies on the synthesis of ZnO nanoparticles (ZnO NPs) using lemon leaves have been reported (12-14). Lemon contains many bioactive components such as citric acid, terpenoid, ascorbic acid, minerals, flavonoids, and essential oils (15). These mentioned properties have recently prompted many researchers to combine them with various compounds, including ZnO, for use in various fields, as lemon leaf extracts have shown to have antimicrobial properties, including bacteria, fungi, and viruses. This can help prevent or treat infections (16). Also, the fabrication of nanoparticles using natural substances helps stabilize the particles, resulting in less toxicity and a greater possibility for reduction. There are several interesting pharmacological effects that ZnO NPs exhibit. In this study, ZnO NPs were synthesized using two different methods: a green method utilizing an inexpensive and readily available leaf extract, and a chemical method. The effectiveness of the resulting nanoparticles was then evaluated against various bacterial species. Additionally, the impact of some currently used antibiotics on the studied bacteria was assessed, and the effectiveness of these antibiotics was compared with that of the ZnO NPs produced in this study.

Materials and Methods

Materials

Lemon leaves were collected from trees growing in Homs, Syria (34°21'N 38°19'E). Pure, high-grade NaOH was supplied by Aldrich Chemicals. Fresh plant leaves of lemon were collected in May 2023 from Homs – Syria. Double-distilled water (DDW) was used in the experiments. The chemical Zinc nitrate hexahydrate (98% purity) used for the analysis was purchased from Merck®. The bacteria used were obtained from the laboratories of Medico Pharmaceutical Industries-Homs-Syria.

Preparation of ZnO nanoparticles

Nano zinc oxide was prepared of ZnO nanoparticles was prepared by green synthesis method in the laboratory of the College of Science - Al-Baath University, using plant extracts (17,18).

Extraction of plant extract

Lemon leaves were washed well with distilled water to clean them of dirt, dust, and other particles. The leaves were then dried at room temperature for a week. Fifty grams of lemon leaves were weighed, and then, cut

into small pieces using a knife. The extract is prepared at a concentration of (50 g in 300 mL distilled water). The extract is then processed by heating at 65 °C for 15 minutes, followed by filtration using a Buchner funnel using Whatman filter paper (No. 1). The resulting solution was saved for the experiment.

Synthesis of ZnO nanoparticles

50 ml of the previously prepared leaf extract was distilled into 100 mL of zinc nitrate dissolved in distilled water (70 mM). The mixture was stirred at 65 °C for 20 minutes. After turning light yellow, it was collected and left in the dryer overnight for 5 days at 65 °C until a yellow powder was obtained. The product was then calcined at 500 °C for 2 hours, then, ground in a mortar before being collected and packaged for the necessary characterization processes. [Figure S1](#) shows the steps of green synthesis of ZnO NPs.

The green synthesis method of nanoparticles is an effective method, where oxidation and reduction are the main reactions, where phytochemicals with antioxidant properties, or microbial enzymes form metal nanoparticles, the main reasons for this method being environmentally friendly are the safe solvents, the reference agent and the non-toxic materials used (19). The basic phytochemicals present in the plant extract, such as terpenoids, flavonoids, and phenolic compounds, contribute to the reduction process. Therefore, the leaf extract's composition significantly affects the synthesis and stabilization of nanoparticles and the amount of nanoparticles produced (20).

The stages of producing green nanoparticles can be explained in the following steps. First, in the activation phase, vegetarian metabolites release metal ions from salt under the influence of their reference work. Zinc ions from the (Zn^{2+}) form are converted to the stable form (Zn^0). In the growth phase, metal atoms are assembled in their stable state as nanoparticles of certain shapes and sizes. Finally, in the completion and stabilization phase, nanoparticles reach their more stable and effective form when they are wrapped up with plant fluctuations (21). [Figure S2](#) shows the stages of manufacturing green nanoparticles.

One of the results obtained when manufacturing ZnO NPs using the green synthesis method is a light-yellow powder precipitate, while the final product of the chemical synthesis method is a white precipitate.

Synthesis of chemical zinc oxide nanoparticles

ZnO NPs were prepared by the wet chemical method through the reaction between zinc nitrate and sodium hydroxide, and soluble starch was used as a stabilizing agent (22).

The First stage: A 1% soluble starch solution was prepared in 1000 mL of distilled water by slight heating at about 20 °C with continuous stirring until a clear solution

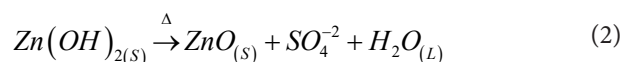
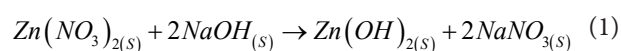
was obtained.

The second stage: 59.49 g of zinc nitrate (0.2 mol) were added to the dissolved starch solution with continuous stirring until we obtained a complete dissolution of zinc nitrate.

The third stage: 0.6 mol of NaOH was added and the drip process was completed within two hours.

The fourth stage: The filtration process was carried out with continuous washing with distilled water to get rid of traces of starch and obtain a white paste.

The fifth stage: The product was dried at 100 °C overnight. During drying, complete zinc hydroxide is converted into ZnO. Then, the process product was collected after the grinding process with a mortar. The steps for the chemical synthesis of nanoparticles are described in Figure 1. The synthesis occurs according to the following equations: (1) Formation mechanism; (2) decomposition mechanism.



Characterization of ZnO NPs

The synthesized ZnO nanoparticles were characterized by a UV-Vis spectrophotometer (Shimadzu, Japan). To obtain the UV-Vis absorption spectrum, the ZnO NPs solution was diluted with distilled water (1:1 ratio) and the spectrum was recorded in the range of 200-500. For FTIR spectroscopy (Shimadzu), the ZnO NPs were transferred using KBr and analyzed. To determine the size and shape of the particles, SEM (VEGA II Xmu, Czech) was used. Finally, X-ray analysis confirmed the presence of ZnO NPs. Powder X-ray diffraction (XRD) (STADI-P STOE, Darmstadt, Germany) equipped with CuK α radiation

($\lambda = 1.54060 \text{ \AA}$) and a germanium monochromator was utilized to explore crystallinity and chemical reaction between crystalline components in the samples. The machine was operated at 50 kV and 30 mA, the XRD patterns were recorded from $2\theta = 10^\circ$ to $2\theta = 90^\circ$ with a scanning step of 0.02° .

Antibacterial activities

The antibacterial activities of ZnO NPs were tested by the agar diffusion method. The following procedure was followed: 100 μL of the bacterial suspension was spread on the surface of the Mueller-Hinton agar medium and refrigerated for 15 minutes to allow the medium to fully absorb. Holes were made in the medium using a sterile glass drill with a diameter of 6 mm, creating 7 holes per dish. Each hole was filled with 100 μL of the prepared ZnO nanoparticles. Gentamycin at a concentration of 30 $\mu\text{g}/\text{mL}$ was used as a positive control. The dishes were refrigerated for two hours to ensure complete absorption. The dishes were then incubated at 37 °C for 24 hours. The average diameter of the inhibition zones was measured using graduated millimeter paper.

Results

Characterization of ZnO nanoparticles

UV-Vis spectroscopy

The absorption spectrum of chemical ZnO NPs is shown in Figure 2a. UV-Visible absorption spectrum of green ZnO NPs is shown in Figure 2b.

Fourier transform infrared spectroscopy (FTIR)

The FTIR spectrum of chemical ZnO NPs is shown in Figure 3a and the FTIR spectrums of the plant extract and the green ZnO NPs are shown in Figures 3b and 3c, respectively. Table 1 shows the comparison between the absorptions of the functional group in the extract and ZnO NPs.

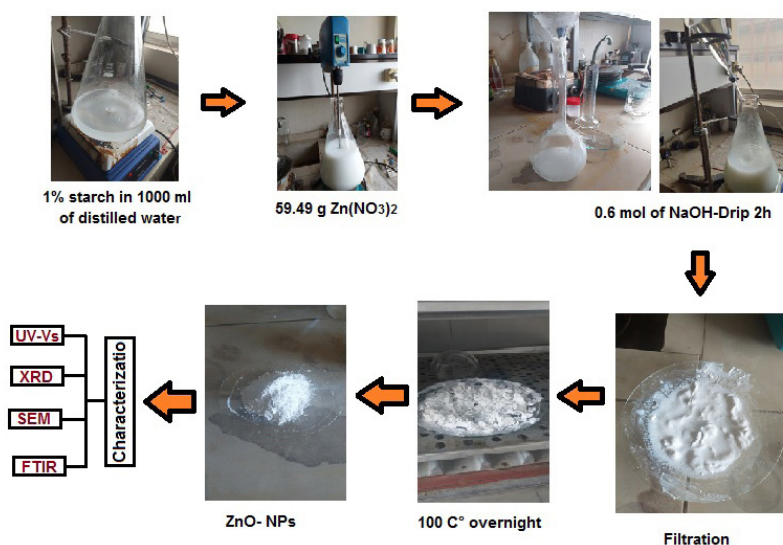


Figure 1. Steps for chemical synthesis of ZnO NPs

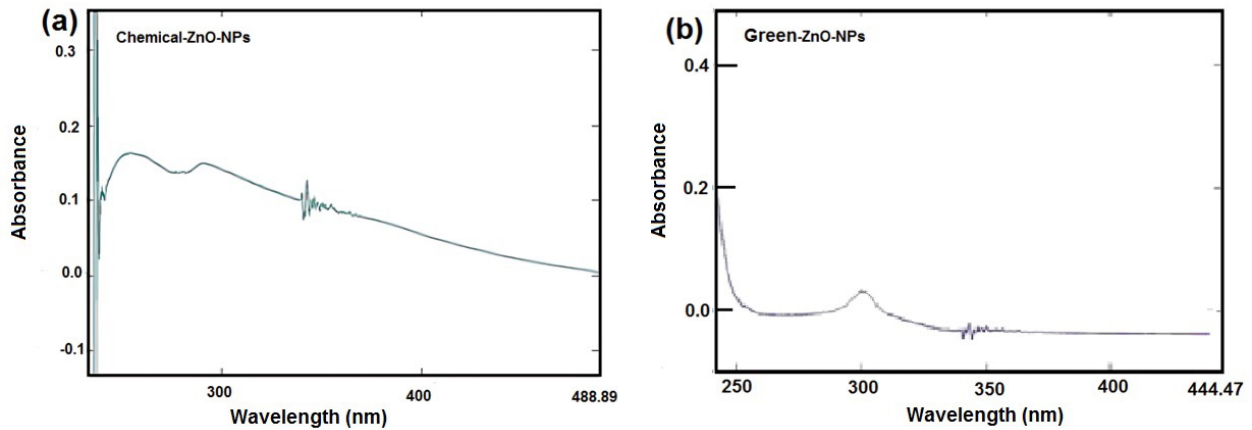


Figure 2. UV-Vis of (a) Chemical ZnO NPs and (b) Green ZnO NPs

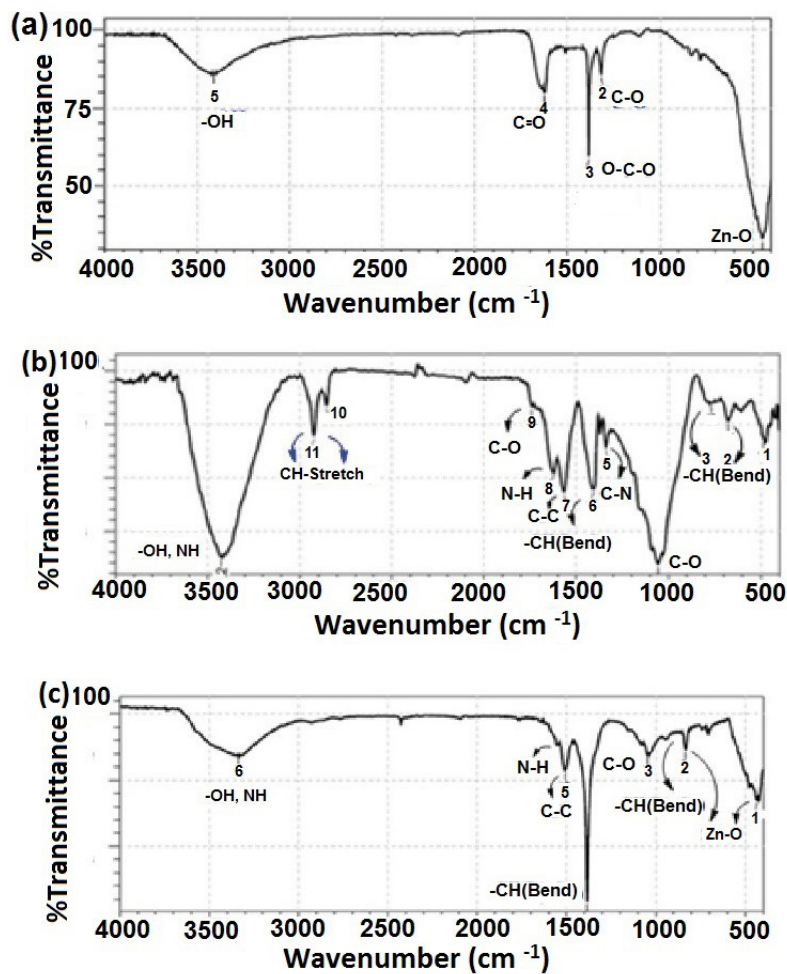


Figure 3. FTIR spectrum diffraction of (a) Chemical ZnO NPs and (b) extract lemon Leave and (c) Green ZnO NPs

X-ray diffraction analysis

The crystalline structure of ZnO NPs was studied by XRD spectrum. The X-ray peaks chemical and green ZnO NPs are shown in Figure 4a and 4b, respectively.

Scanning electron microscope (SEM)

The SEM analysis was performed to determine the shape and morphology of ZnO NPs (Figure 5).

Antibacterial activity

To test the effectiveness of ZnO nanoparticles against bacterial activity, the development of bacterial activity

by *S. aureus*, *E. coli*, and *P. aeruginosa* in the presence of different concentrations of ZnO nanoparticles was studied. The effective results of green ZnO nanoparticles and chemical ZnO nanoparticles are summarized in Tables 2 and 3. The diameters of the undeveloped corona (in nm) are shown in Figure 6.

Discussion

The absorption spectrum of chemical ZnO NPs is shown in Figure 2a. It exhibits a strong absorption band at about 289 nm. An excitonic absorption peak is found at about

258 nm.

It is also evident that the UV-Visible absorption spectrum of green ZnO NPs is shown in Figure 2b. The distinct peak centered about 301 nm. These peaks fall within the range of ZnO nanoparticle absorption, confirming the identity of the formed ZnO nanoparticles, which is consistent with the results of some studies (23,24). The FTIR spectrum of the chemical ZnO NPs is shown in Figure 3a, where there is a strong and broad absorption peak at 3420 cm^{-1} that corresponds to the vibrations of the -O-H groups as the O-H may belong to the phenolic compounds.

One significant peak at 450 cm^{-1} was seen in the FTIR spectrum, which belongs to Zn-O, which is consistent with the results of other reports (25), a different stretching vibrational mode of ZnO was observed. Additional bands are seen between $800\text{-}900\text{ cm}^{-1}$, which is attributed to the C-H bend (26). The bands between $1600\text{-}1300\text{ cm}^{-1}$ are associated with the C=O and the O-C-O bonds (27).

As shown in Figure 3b, FT-IR analysis helped identify the functional groups present in the plant extract that contribute to the binding mechanism with ZnO NPs. Lemon leaves extract contains a high percentage of polyphenolic derivatives such as flavonoids, anthocyanins, terpenoids, and cyanidin-3-glucoside, which are considered potential bioactive compounds for treatments and to act as reducing agents.

Table 1. Comparison between the absorptions of the functional group in the extract and ZnO NPs

ZnO NPs	Wave Number $\nu(\text{Cm}^{-1})$	
	The extract	Functional group
3340	3450	O-H, NH_2 (Stretch)
-	2925, 2850	-CH (Stretch) symmetric and asymmetric
-	1750	C=O
1590	1650	N-H
1540	1580	C=C
1390	1425	-CH(Bend)
-	1325	C-N(amines)
1040	1050	C-O
950	800- 900	=CH(Bend)

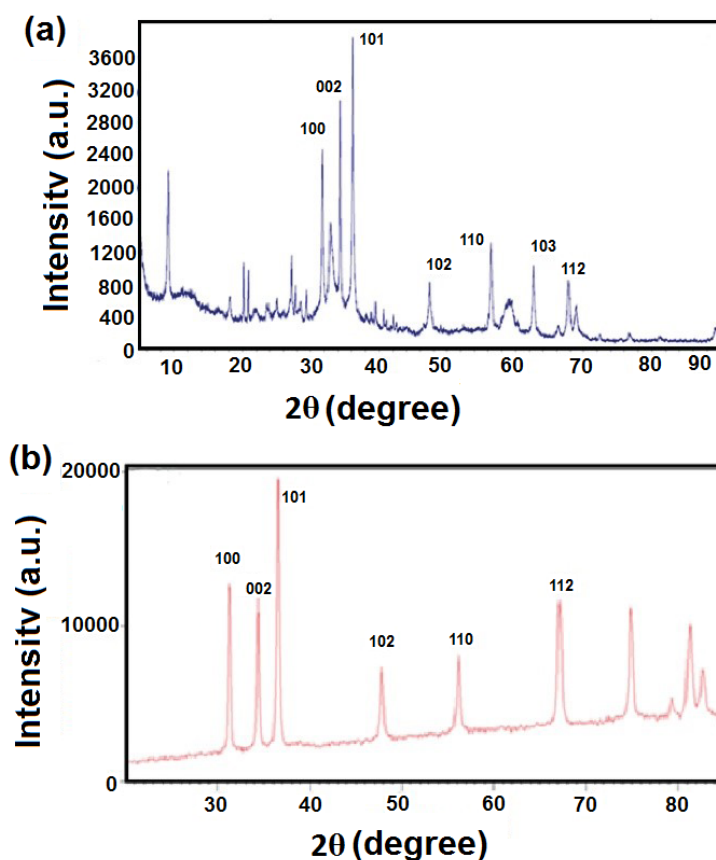


Figure 4. X-ray diffraction spectrum of ZnO NPs (a) chemical ZnO NPs and (b) green ZnO NPs

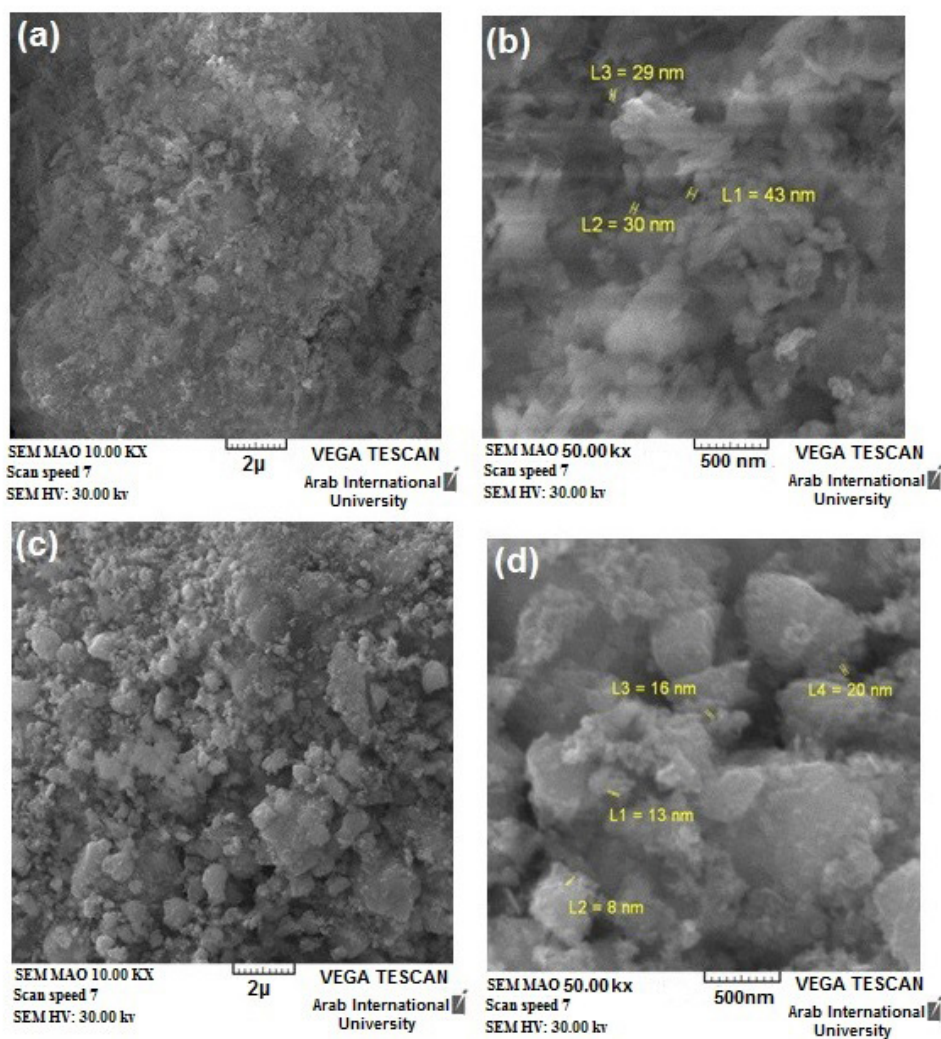


Figure 5. SEM images at 10 and 50 KX of (a and b) Chemical ZnO NPs and (c and d) Green ZnO NPs, respectively

Table 2. The effectiveness of chemical ZnO NPs against bacteria

The Germ	Diameters of the non-growth halo (in mm)						
	Concentration						
	Gentamicin (Control)	200 mg/mL (1)	100 mg/mL (2)	50 mg/mL (3)	25 mg/mL (4)	12,5 mg/mL (5)	6,25 mg/mL (6)
<i>Staphylococcus aureus</i>	20.1	19	17.1	15.1	13	–	–
<i>Escherichia coli</i>	16.2	13.1	11	–	–	–	–
<i>Pseudomonas aeruginosa</i>	13.1	13.6	12.4	11	–	–	–

Table 3. The effects of green ZnO NPs against bacteria

The Germ	Diameters of the non-growth halo (in mm)						
	Concentration						
	Gentamicin (Control)	200 mg/mL (1)	100 mg/mL (2)	50 mg/mL (3)	25 mg/mL (4)	12,5 mg/mL (5)	6,25 mg/mL (6)
<i>Staphylococcus aureus</i>	20.1	21.1	20	17.1	16.1	15.1	12
<i>Escherichia coli</i>	16.2	12.3	11.2	–	–	–	–
<i>Pseudomonas aeruginosa</i>	13.1	13	–	–	–	–	–

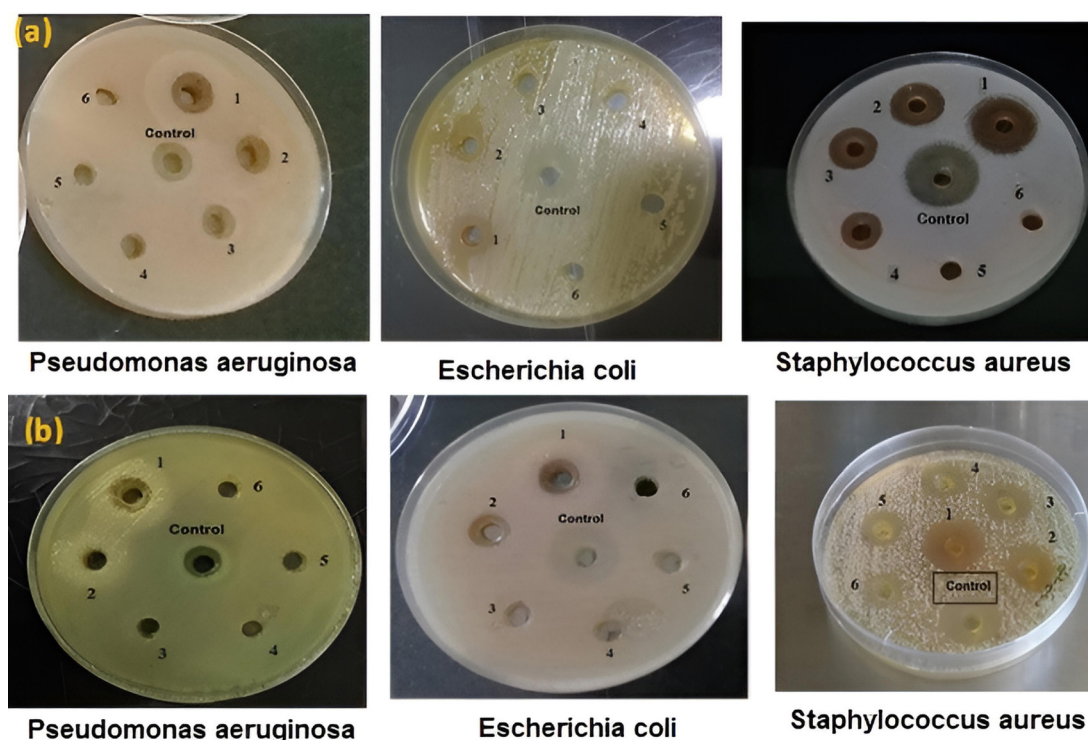


Figure 6. Diameters of the non-growth halo (in mm) of chemical ZnO NPs (a) and green ZnO NPs (b)

Accordingly, the FT-IR spectrum of the plant extract exhibited several peaks at 3450, 2925, 2850, 1750, 1650, 1580, 1410, 1380, 1325, 1200, and 1080 cm^{-1} . The peaks at 3450 (O-H) and $-\text{NH}_2$ groups, 1580–1650 (N-H), and 1080 (C-O) or 800–1380 (RCOO) cm^{-1} are related to alkaloids, flavonoids, and phenolic compounds, respectively (28).

FT-IR spectra of the biosynthesized ZnO NPs (Figure 3c) showed a small shift with slight changes in some related peaks. The major peaks of the plant extract shifting from 3450 to 3340 cm^{-1} in ZnO were assigned to the O-H of the phenol groups and $-\text{NH}_2$, while another peak shifted from 1650 to 1590 cm^{-1} was ascribed to binding N-H.

The double bond between the bands (1500–1600) cm^{-1} indicates the presence of terpenoids (29–31). Furthermore, the FTIR spectrum of the biosynthesized ZnO NPs showed a sharp and intense band at 450 cm^{-1} (32), indicating the existence of Zn-O vibrations (33). It is worth noting that any peak in the range of 400–600 cm^{-1} is a characteristic peak for nano ZnO (metal oxides) (34). The FTIR results demonstrated that phenol, flavonoid, terpenoids, and amines present in the extract might have been involved in the formation of ZnO NPs from Zn (NO_3)₂ as the reductant agent. Table 1 shows the comparison between the absorptions of the functional group in the extract and ZnO NPs.

As shown in Figure 4a, the XRD diffraction of chemical ZnO NPs peaks showed at 2θ angles of 31.8°, 34.3°, 36.2°, 48°, 56.6°, 62.76°, and 67° corresponding to lattice planes (100), (002), (101), (102), (110), (103), and (112),

respectively. Likewise, the XRD diffraction of green ZnO NPs peaks showed at 2θ angles of 31.3°, 34.45°, 36.7°, 48°, 56°, and 67° corresponding to lattice planes (100), (002), (101), (102), (110), and (112), respectively (Figure 4b). The peaks were matched to ICDD card number 01-079-0207 (35,36).

The additional peaks in the nano chemical sample indicate that the sample is not pure and contains impurities due to the chemical not calcifying compared to the green synthetic ZnO nanoparticle pattern.

It can be concluded from the figure that the sharp and narrow diffraction peaks indicate that the product has a good crystalline nature. It was revealed that the XRD peaks resulting from the green synthesis method are not as sharp as those found in the chemical synthesis method, which indicates the synthesis of smaller-sized particles. It can also be observed that the amplitudes of the peaks from the green synthesis method using lemon leaf extract were larger compared to those from the chemical synthesis method, indicating that the green synthesized molecules have smaller particle sizes (37,38). This result was confirmed by scanning electron microscopic analysis of the dimensions of the manufactured nanoparticles, as the size of the particles manufactured using the chemical synthesis method was larger (34 nm) than those manufactured using the green synthesis method (14.25 nm).

The SEM image of chemical ZnO NPs were nearly almost-spherical shapes and heterogeneous where the average particle size was 34 nm, as shown in Figures 5a and b.

Scanning electron microscope images of the green

synthesis nanoparticles revealed well-dispersed spherical particles with an average size of 14.25 nm, as shown in Figures 5c and 5d.

It can be explained that the particle size of green synthesized ZnO NPs is relatively smaller than that of chemically synthesized nanoparticles. This can be also caused due to the presence of phenol, flavonoids, terpenoids, and amines in the lemon leaf extract as a powerful reducing agent interacts with ZnO NPs and reduces its size significantly (39,40).

As shown in Table 2, all isolates exhibited sensitivity to ZnO NPs -chemical (Figure 6a). *Staphylococcus aureus* was the most sensitive, within concentrations of 25–200 mg /mL with growth inhibition halo diameters ranging 13–19 mm at concentrations of 200 mg /mL compared to Gentamycin (20.1) mm, followed by *Escherichia coli*, which responded only at concentrations of 100–200 mg /mL and with growth inhibition halo diameters of 11–13.1 mm, while *P. aeruginosa* was affected only within concentrations of 50–200 mg /mL with growth inhibition halo diameters ranging 11–13.6 mm, and the lower concentrations also had no significant effect.

Table 3 and Figure 6b also showed that all the studied bacteria showed sensitivity towards green ZnO NPs. *S. aureus* was the most sensitive, responding to nano ZnO at all studied concentrations with growth inhibition halo diameters ranging 12–21.1 mm. This was followed by *E. coli*, which responded at concentrations of 100–200 mg /mL with diameters reaching 11.2–12.3 mm, respectively. *Pseudomonas aeruginosa* was affected only at a concentration of 200 mg/mL with a diameter of 13 mm, while the lower concentrations had no effect. This is consistent with the results of several studies (41–43). The difference between these studies is due to the manufacturing method used, which gives different nanoscopic dimensions, which in turn affects the antibacterial effectiveness. We can explain the results as a result of the difference in the properties of the material when reaching the nano-size, and the most important of these properties is its antibacterial effectiveness (44,45). As the specific surface area of the particles increases when changing to the nano-size, the surface oxygen concentration increases, thus, increasing its association with the germs and its destruction of the cytoplasmic membrane and the bacterial cell wall. The so-called oxidative stress is based on oxygen free radicals (46), and there is another proposed mechanism that is due to the direct effect of ZnONPs on the cell wall of bacteria as a result of the attraction between the overall positively charged nanoparticles and the capsule composed of negatively charged polysaccharides, which causes cell encapsulation with high concentrations of ZnO NPs (47,48), which in turn are generated by reactive oxygen radicals, especially hydroxyl radicals, within the surrounding aqueous environment. These radicals, which interact significantly

with all compounds and cellular structures, cause cell wall erosion and facilitate the penetration of nanoparticles at high concentrations. Large quantities enter the cell (49), where zinc ions begin to be released more under the influence of the acidic environment of lysosomes inside the cell. These high concentrations cause cytotoxicity due to the inhibition of respiratory chain enzymes, and thus, induction of apoptosis (50,51).

The comparison of the effectiveness of ZnO nanoparticles manufactured by the green synthesis method with those manufactured chemically showed that the preference is clearly and significantly given to the particles manufactured by the green synthesis method. This may be explained by the fact that the particles, when manufactured by two different methods, possessed different properties, the most important of which is their size. The size of the particles manufactured by the chemical synthesis method was larger (34 nm) than the particles manufactured using the green synthesis method (14.25 nm), therefore, the size is an important and decisive factor in the antibacterial effect (52).

Conclusion

According to the results of this study, green synthesis could be a favorable method for synthesizing ZnO NPs compared to chemical synthesis. The obtained ZnO was characterized through UV, XRD, SEM, and FT-IR analysis. The absorption spectrum of ZnO NPs-Chemical shows a strong absorption band at about 289 nm compared to ZnO NPs-Green with an absorption band of about 301 nm. The average size of the ZnO NPs-Green was 14.25 nm smaller than that of the ZnO NPs-Chemical at 34 nm.

The antibacterial activity of ZnO NPs was evaluated on two gram-negative bacterial strains, *E. coli* and *P. aeruginosa*, and a gram-positive strain (*S. aureus*), by studying their effectiveness and using gentamicin as a control. Green ZnO NPs suspensions showed stronger antibacterial activity against *S. aureus* at all concentrations, with inhibition diameters ranging from 12 to 21.1 mm, and responded to *P. aeruginosa* only at concentrations of 200 mg /mL, with an average growth inhibition halo of 13 mm. ZnO NPs-Chemical showed clear activity against *P. aeruginosa* at concentrations of 50–200 mg /mL and with growth inhibition diameters ranging 11–13.6 mm, but responded to *S. aureus* only at concentrations of 25–200 mg /mL and with inhibition diameters ranging 13–19 mm.

Acknowledgements

The authors are grateful to Al-Baath University for supporting this research.

Authors' contributions

Conceptualization: Hassan Abbas.

Data curation: Arwa AlBustany.

Formal analysis: Arwa AlBustany.

Investigation: Arwa AlBustany and Thanaa Shriteh.

Methodology: Abd Al-Naser Al-Omar.

Project administration: Hashem AL Mahfoud.

Supervision: Hassan Abbas and Abd Al-Naser Al-Omar.

Validation: Alaa Sobh.

Visualization: No Applicable.

Writing–original draft: Arwa AlBustany.

Writing–review & editing: Alaa Sobh.

Competing interests

The authors declare that they have no conflict of interests regarding the publication of the present article.

Ethical issues

Not applicable.

Funding

Not applicable.

Supplementary files

Supplementary file 1 contains Figures S1 and S2.

References

- Sharmila G, Muthukumaran C, Sangeetha E, Saraswathi H, Soundarya S, Kumar NM. Green fabrication, characterization of *Pisonia alba* leaf extract derived MgO nanoparticles and its biological applications. *Nano-Struct Nano-Objects*. 2019;20:100380. doi: [10.1016/j.nanos.2019.100380](https://doi.org/10.1016/j.nanos.2019.100380).
- Soubh AM, Abdoli MA, Ahmad LA. Optimizing the removal of methylene blue from aqueous solutions using persulfate activated with nanoscale zero-valent iron (nZVI) supported by reduced expanded graphene oxide (rEGO). *Environ Health Eng Manag*. 2021;8(1):15-24. doi: [10.34172/ehem.2021.03](https://doi.org/10.34172/ehem.2021.03).
- Iravani S. Bacteria in nanoparticle synthesis: current status and future prospects. *Int Sch Res Notices*. 2014;2014:359316. doi: [10.1155/2014/359316](https://doi.org/10.1155/2014/359316).
- Soubh AM. The performance of iron nanocomposites as persulfate activators in permeable reactive barrier technology for treatment of landfill leachate. *Avicenna J Environ Health Eng*. 2024;11(1):1-11. doi: [10.34172/ajehe.5428](https://doi.org/10.34172/ajehe.5428).
- Zhang X, Guo Q, Cui D. Recent advances in nanotechnology applied to biosensors. *Sensors (Basel)*. 2009;9(2):1033-53. doi: [10.3390/s90201033](https://doi.org/10.3390/s90201033).
- Alijani K, Rezaei J, Rouzbehan Y. Effect of nano-ZnO, compared to ZnO and Zn-methionine, on performance, nutrient status, rumen fermentation, blood enzymes, ferric reducing antioxidant power and immunoglobulin G in sheep. *Anim Feed Sci Technol*. 2020;267:114532. doi: [10.1016/j.anifeedsci.2020.114532](https://doi.org/10.1016/j.anifeedsci.2020.114532).
- Tan LF, Yap VL, Rajagopal M, Wiart C, Selvaraja M, Leong MY, et al. Plant as an alternative source of antifungals against *Aspergillus* infections: a review. *Plants (Basel)*. 2022;11(22):3009. doi: [10.3390/plants11223009](https://doi.org/10.3390/plants11223009).
- Chang YN, Zhang M, Xia L, Zhang J, Xing G. The toxic effects and mechanisms of CuO and ZnO nanoparticles. *Materials (Basel)*. 2012;5(12):2850-71. doi: [10.3390/ma5122850](https://doi.org/10.3390/ma5122850).
- Luo Z, Wu Q, Xue J, Ding Y. Selectively enhanced antibacterial effects and ultraviolet activation of antibiotics with ZnO nanorods against *Escherichia coli*. *J Biomed Nanotechnol*. 2013;9(1):69-76. doi: [10.1166/jbn.2013.1472](https://doi.org/10.1166/jbn.2013.1472).
- Youn SM, Choi SJ. Food additive zinc oxide nanoparticles: dissolution, interaction, fate, cytotoxicity, and oral toxicity. *Int J Mol Sci*. 2022;23(11):6074. doi: [10.3390/ijms23116074](https://doi.org/10.3390/ijms23116074).
- Oyetola EO. Comparative studies of biosynthesized zinc oxide nanoparticles. *Nanochem Res*. 2023;8(1):31-9. doi: [10.22036/ncr.2023.01.003](https://doi.org/10.22036/ncr.2023.01.003).
- Rafique M, Sohaib M, Tahir R, Tahir MB, Khalid NR, Shakil M, et al. Novel, facile and first time synthesis of zinc oxide nanoparticles using leaves extract of *Citrus reticulata* for photocatalytic and antibacterial activity. *Optik*. 2021;243:167495. doi: [10.1016/j.ijleo.2021.167495](https://doi.org/10.1016/j.ijleo.2021.167495).
- El-Arab NB. Synthesis and characterization of zinc oxide nanoparticles using green and chemical synthesis techniques for phenol decontamination. *Int J Nanoel*. 2018;11(2):179-94.
- Thongam DD, Chaturvedi H. Effect of biochemical compounds on ZnO nanomaterial preparation using *Aloe vera* and lemon extracts. *Mater Today Proc*. 2021;44(Pt 6):4299-304. doi: [10.1016/j.matpr.2020.10.548](https://doi.org/10.1016/j.matpr.2020.10.548).
- Di Vaio C, Graziani G, Gaspari A, Scaglione G, Nocerino S, Ritieni A. Essential oils content and antioxidant properties of peel ethanol extract in 18 lemon cultivars. *Sci Hortic*. 2010;126(1):50-5. doi: [10.1016/j.scienta.2010.06.010](https://doi.org/10.1016/j.scienta.2010.06.010).
- Waliwita WA, Dharshika AK, Liyanage RP, Dissanayake KG. Pharmacological actions of *Citrus limon* leaves. *Int J All Res Educ Sci Methods*. 2021;9(3):1760-6.
- Nayak R, Ali FA, Mishra DK, Ray D, Aswal VK, Sahoo SK, et al. Fabrication of CuO nanoparticle: an efficient catalyst utilized for sensing and degradation of phenol. *J Mater Res Technol*. 2020;9(5):11045-59. doi: [10.1016/j.jmrt.2020.07.100](https://doi.org/10.1016/j.jmrt.2020.07.100).
- Nawaz HR, Solangi BA, Zehra B, Nadeem U. Preparation of nano zinc oxide and its application in leather as a retanning and antibacterial agent. *Can J Sci Ind Res*. 2011;2(4):164-70.
- Singh J, Dutta T, Kim KH, Rawat M, Samddar P, Kumar P. 'Green' synthesis of metals and their oxide nanoparticles: applications for environmental remediation. *J Nanobiotechnology*. 2018;16(1):84. doi: [10.1186/s12951-018-0408-4](https://doi.org/10.1186/s12951-018-0408-4).
- Mukunthan KS, Balaji S. Cashew apple juice (*Anacardium occidentale* L.) speeds up the synthesis of silver nanoparticles. *Int J Green Nanotechnol*. 2012;4(2):71-9. doi: [10.1080/19430892.2012.676900](https://doi.org/10.1080/19430892.2012.676900).
- Panchakarla LS, Govindaraj A, Rao CNR. Formation of ZnO nanoparticles by the reaction of zinc metal with aliphatic alcohols. *J Clust Sci*. 2007;18(3):660-70. doi: [10.1007/s10876-007-0129-6](https://doi.org/10.1007/s10876-007-0129-6).
- Yadav A, Prasad V, Kathe AA, Raj S, Yadav D, Sundaramoorthy C, et al. Functional finishing in cotton fabrics using zinc oxide nanoparticles. *Bull Mater Sci*. 2006;29(6):641-5. doi: [10.1007/s12034-006-0017-y](https://doi.org/10.1007/s12034-006-0017-y).
- Jayarambabu N, Kumari BS, Rao KV, Prabhu YT. Germination and growth characteristics of mungbean seeds (*Vigna radiata* L.) affected by synthesized zinc oxide nanoparticles. *Int J Curr Eng Technol*. 2014;4(5):3411-6.
- Navale GR, Thripuranthaka M, Late DJ, Shinde SS. Antimicrobial activity of ZnO nanoparticles against pathogenic bacteria and fungi. *JSM Nanotechnol Nanomed*. 2015;3(1):1033.
- Zandi S, Kameli P, Salamati H, Ahmadvand H, Hakimi M. Microstructure and optical properties of ZnO nanoparticles prepared by a simple method. *Physica B Condens Matter*. 2011;406(17):3215-8. doi: [10.1016/j.physb.2011.05.026](https://doi.org/10.1016/j.physb.2011.05.026).
- Chouhan S, Bajpai AK, Bajpai J, Katare R, Dhoble SJ. Mechanical and UV absorption behavior of zinc oxide

- nanoparticles: reinforced poly(vinyl alcohol-g-acrylonitrile) nanocomposite films. *Polym Bull.* 2017;74(10):4119-41. doi: [10.1007/s00289-017-1942-1](https://doi.org/10.1007/s00289-017-1942-1).
27. Senthilkumar N, Nandhakumar E, Priya P, Soni D, Vimalan M, Vetha Potheher I. Synthesis of ZnO nanoparticles using leaf extract of *Tectona grandis* (L.) and their anti-bacterial, anti-arthritis, anti-oxidant and in vitro cytotoxicity activities. *New J Chem.* 2017;41(18):10347-56. doi: [10.1039/c7nj02664a](https://doi.org/10.1039/c7nj02664a).
 28. Ganesh M, Lee SG, Jayaprakash J, Mohankumar M, Jang HT. *Hydnocarpus alpina* Wt extract mediated green synthesis of ZnO nanoparticle and screening of its antimicrobial, free radical scavenging, and photocatalytic activity. *Biocatal Agric Biotechnol.* 2019;19:101129. doi: [10.1016/j.bcab.2019.101129](https://doi.org/10.1016/j.bcab.2019.101129).
 29. Hu D, Si W, Qin W, Jiao J, Li X, Gu X, et al. Cucurbita pepo leaf extract induced synthesis of zinc oxide nanoparticles, characterization for the treatment of femoral fracture. *J Photochem Photobiol B.* 2019;195:12-6. doi: [10.1016/j.jphotobiol.2019.04.001](https://doi.org/10.1016/j.jphotobiol.2019.04.001).
 30. Sirdeshpande KD, Sridhar A, Cholkar KM, Selvaraj R. Structural characterization of mesoporous magnetite nanoparticles synthesized using the leaf extract of *Calliandra haematocephala* and their photocatalytic degradation of malachite green dye. *Appl Nanosci.* 2018;8(4):675-83. doi: [10.1007/s13204-018-0698-8](https://doi.org/10.1007/s13204-018-0698-8).
 31. Lu J, Batjikh I, Hurh J, Han Y, Ali H, Mathiyalagan R, et al. Photocatalytic degradation of methylene blue using biosynthesized zinc oxide nanoparticles from bark extract of *Kalopanax septemlobus*. *Optik.* 2019;182:980-5. doi: [10.1016/j.ijleo.2018.12.016](https://doi.org/10.1016/j.ijleo.2018.12.016).
 32. Stan M, Popa A, Toloman D, Silipas TD, Vodnar DC. Antibacterial and antioxidant activities of ZnO nanoparticles synthesized using extracts of *Allium sativum*, *Rosmarinus officinalis* and *Ocimum basilicum*. *Acta Metall Sin (Engl Lett).* 2016;29(3):228-36. doi: [10.1007/s40195-016-0380-7](https://doi.org/10.1007/s40195-016-0380-7).
 33. Taghavi Fardood S, Ramazani A, Moradi S, Azimzadeh Asiabi P. Green synthesis of zinc oxide nanoparticles using arabic gum and photocatalytic degradation of direct blue 129 dye under visible light. *J Mater Sci Mater Electron.* 2017;28(18):13596-601. doi: [10.1007/s10854-017-7199-5](https://doi.org/10.1007/s10854-017-7199-5).
 34. Handore K, Bhavsar S, Horne A, Chhattise P, Mohite K, Ambekar J, et al. Novel green route of synthesis of ZnO nanoparticles by using natural biodegradable polymer and its application as a catalyst for oxidation of aldehydes. *J Macromol Sci Part A.* 2014;51(12):941-7. doi: [10.1080/10601325.2014.967078](https://doi.org/10.1080/10601325.2014.967078).
 35. Vinayagam R, Selvaraj R, Arivalagan P, Varadavenkatesan T. Synthesis, characterization and photocatalytic dye degradation capability of *Calliandra haematocephala*-mediated zinc oxide nanoflowers. *J Photochem Photobiol B.* 2020;203:111760. doi: [10.1016/j.jphotobiol.2019.111760](https://doi.org/10.1016/j.jphotobiol.2019.111760).
 36. Bhasha S, Malik P, Santosh S, Purnima J. Synthesis and characterization of nanocrystalline zinc oxide thin films for ethanol vapor sensor. *J Nanomed Nanotechnol.* 2015;6(4):306. doi: [10.4172/2157-7439.1000306](https://doi.org/10.4172/2157-7439.1000306).
 37. Elkady MF, El-Sayed EM, Farag HA, Zaatout AA. Assessment of novel synthesized nanozirconium tungstovanadate as cation exchanger for lead ion decontamination. *J Nanomater.* 2014;2014(1):149312. doi: [10.1155/2014/149312](https://doi.org/10.1155/2014/149312).
 38. Karam ST, Abdulrahman AF. Green synthesis and characterization of ZnO nanoparticles by using thyme plant leaf extract. *Photonics.* 2022;9(8):594. doi: [10.3390/photonics9080594](https://doi.org/10.3390/photonics9080594).
 39. de Passos MS, de Carvalho Junior AR, Boeno SI, de Lima Glória das Virgens L, Calixto SD, Ventura TL, et al. Terpenoids isolated from *Azadirachta indica* roots and biological activities. *Rev Bras Farmacogn.* 2019;29(1):40-5. doi: [10.1016/j.bjp.2018.12.003](https://doi.org/10.1016/j.bjp.2018.12.003).
 40. Mwafy A, Youssef DY, Mohamed MM. Antibacterial activity of zinc oxide nanoparticles against some multidrug-resistant strains of *Escherichia coli* and *Staphylococcus aureus*. *Int J Vet Sci.* 2023;12(3):284-8. doi: [10.47278/journal.ijvs/2022.181](https://doi.org/10.47278/journal.ijvs/2022.181).
 41. Gao Y, Xu D, Ren D, Zeng K, Wu X. Green synthesis of zinc oxide nanoparticles using *Citrus sinensis* peel extract and application to strawberry preservation: a comparison study. *LWT.* 2020;126:109297. doi: [10.1016/j.lwt.2020.109297](https://doi.org/10.1016/j.lwt.2020.109297).
 42. Ismail SN, Abd AN, Dakhil OA. Comparison of ZnO nanoparticles by chemical and aqueous hydrolysis and evaluation of their antibacterial activity. *Plant Arch.* 2020;20:3372-6.
 43. Sajanlal PR, Sreeprasad TS, Samal AK, Pradeep T. Anisotropic nanomaterials: structure, growth, assembly, and functions. *Nano Rev.* 2011;2(1):5883. doi: [10.3402/nano.v2i0.5883](https://doi.org/10.3402/nano.v2i0.5883).
 44. Vega-Jiménez AL, Vázquez-Olmos AR, Acosta-Gío E, Álvarez-Pérez MA. In vitro antimicrobial activity evaluation of metal oxide nanoparticles. In: Koh KS, Wong VL, eds. *Nanoemulsions - Properties, Fabrications and Applications*. IntechOpen; 2019. p. 1-8. doi: [10.5772/intechopen.84369](https://doi.org/10.5772/intechopen.84369).
 45. Yazdanpanah G, Javid N, Honarmandrad Z, Amirmahani N, Nasiri A. Evaluation of antimicrobial activities of powdered cuttlebone against *Klebsiella oxytoca*, *Staphylococcus aureus*, and *Aspergillus flavus*. *Environ Health Eng Manag.* 2021;8(1):39-45. doi: [10.34172/ehem.2021.06](https://doi.org/10.34172/ehem.2021.06).
 46. Mendes CR, Dilari G, Forsan CF, de Moraes Ruy Sapata V, Lopes PR, de Moraes PB, et al. Antibacterial action and target mechanisms of zinc oxide nanoparticles against bacterial pathogens. *Sci Rep.* 2022;12(1):2658. doi: [10.1038/s41598-022-06657-y](https://doi.org/10.1038/s41598-022-06657-y).
 47. Lallo da Silva B, Abuçafy MP, Berbel Manaia E, Oshiro Junior JA, Chiari-Andréo BG, Pietro RC, et al. Relationship between structure and antimicrobial activity of zinc oxide nanoparticles: an overview. *Int J Nanomedicine.* 2019;14:9395-410. doi: [10.2147/ijn.s216204](https://doi.org/10.2147/ijn.s216204).
 48. Baysal A, Saygin H, Ustabasi GS. Physicochemical transformation of ZnO and TiO₂ nanoparticles in sea water and its impact on bacterial toxicity. *Environ Health Eng Manag.* 2019;6(1):73-80. doi: [10.15171/ehem.2019.08](https://doi.org/10.15171/ehem.2019.08).
 49. Siddiqi KS, Ur Rahman A, Tajuddin, Husen A. Properties of zinc oxide nanoparticles and their activity against microbes. *Nanoscale Res Lett.* 2018;13(1):141. doi: [10.1186/s11671-018-2532-3](https://doi.org/10.1186/s11671-018-2532-3).
 50. Jiang Y, Zhang L, Wen D, Ding Y. Role of physical and chemical interactions in the antibacterial behavior of ZnO nanoparticles against *E. coli*. *Mater Sci Eng C Mater Biol Appl.* 2016;69:1361-6. doi: [10.1016/j.msec.2016.08.044](https://doi.org/10.1016/j.msec.2016.08.044).
 51. Mishra PK, Mishra H, Ekielski A, Talegaonkar S, Vaidya B. Zinc oxide nanoparticles: a promising nanomaterial for biomedical applications. *Drug Discov Today.* 2017;22(12):1825-34. doi: [10.1016/j.drudis.2017.08.006](https://doi.org/10.1016/j.drudis.2017.08.006).
 52. Jayachandran A, T RA, Nair AS. Green synthesis and characterization of zinc oxide nanoparticles using *Cayratia pedata* leaf extract. *Biochem Biophys Rep.* 2021;26:100995. doi: [10.1016/j.bbrep.2021.100995](https://doi.org/10.1016/j.bbrep.2021.100995).